

Real-space Condensation in Stochastic Mass Transport Models

Satya N. Majumdar

*Laboratoire de Physique Théorique et Modèles Statistiques,
Université Paris-Sud. Bât. 100. 91405 Orsay Cedex. France*

The phenomenon of real-space condensation is encountered in a variety of situations such as aggregation and fragmentation processes, granular clustering, phase separation, traffic and networks. Unlike traditional Bose-Einstein condensation in the *momentum space*, a condensate in these systems forms in *real space*, e.g., upon increasing the density beyond a critical value a macroscopically large mass/cluster may form at a single site on a lattice. In this brief review, I discuss some recent developments in understanding the physical and mathematical mechanism behind this real-space condensation in a class of simple stochastic mass transport models.

I. INTRODUCTION

The phenomenon of Bose-Einstein condensation (BEC) in an ideal Bose gas is by now a textbook material and has recently seen a huge revival of interest driven mostly by new experiments. Consider an ideal gas of N bosons in a d -dimensional hypercubic box of volume $V = L^d$. In the thermodynamic limit $N \rightarrow \infty$, $V \rightarrow \infty$ but with the density $\rho = N/V$ fixed, as one reduces the temperature below a certain critical value $T_c(\rho)$ in $d > 2$, macroscopically large number of particles ($\propto V$) condense on to the ground state, i.e., in the zero momentum quantum state. Alternately, one encounters the same condensation transition upon fixing the temperature but increasing the density ρ beyond a critical value $\rho_c(T)$.

The traditional BEC happens in the momentum (or equivalently energy) space. In contrast, over the last two decades it has been realized that a ‘similar’ Bose-Einstein type condensation can also occur in *real space* in the steady state of a variety of nonequilibrium systems such as in cluster aggregation and fragmentation [1], jamming in traffic and granular flow [2, 3] and granular clustering [4]. The common characteristic feature that these systems share is the stochastic transport of some conserved scalar quantity which can simply be called mass. Condensation transition in these systems occurs when above some critical mass density a single ‘condensate’ captures a finite fraction of the total mass of the system. ‘Condensate’ corresponds to a dominant cluster in the context of granular clustering, or a single large jam in the context of traffic models. Another example of condensation is found in the phase separation dynamics in one dimensional driven systems where the condensation manifests itself in the emergence of a macroscopic domain of one phase [5]. Other examples of such real-space condensation can be found in the socioeconomic contexts: for example, in wealth condensation in macroeconomics where a single individual or a company (condensate) owns a finite fraction of the total wealth [6] or in growing networks where a single node or hub (such as ‘google’) may capture a finite fraction of links in the network [7].

This real-space condensation mentioned above has been studied theoretically in very simple stochastic mass transport models defined on lattices. These are typically nonequilibrium models without any Hamiltonian and are defined by their microscopic dynamical rules that specify how some scalar quantities such as masses or a certain number of particles get transported from site to site of the lattice. These rules typically violate detailed balance [8]. Under these rules, the system evolves into a *stationary* or *steady* state which are typically not Gibbs-Boltzmann state as the system lacks a Hamiltonian [8]. For a class of transport rules, the system can reach a steady state where upon increasing the density of mass or particles beyond a critical value, a macroscopically large mass (or number of particles) condenses onto a single site of the lattice, signalling the onset of ‘real-space’ condensation.

In this article we will mostly focus on *homogeneous* systems where the transport rules are independent of sites, i.e., the system is translationally invariant. In the condensed phase and in an infinite system, the condensate forms at a single site which thus breaks the translational invariance spontaneously. In a finite system, the condensate at a given site has a finite lifetime beyond which it dissolves and then gets relocated at a different site and the various time scales associated with the formation/relocation of the condensate diverge with the increasing system size (see later). In *heterogeneous* systems where the transport rules may differ from site to site, the condensate may form at a site with the lowest outgoing mass transport rate [9, 10, 11]. The mechanism of the condensation transition in such heterogeneous systems is exactly analogous to the traditional BEC in momentum space and the site with the lowest outgoing mass transfer rate plays the role of the ground state in the quantum system of ideal Bose gas. In contrast, the mechanism of condensation in homogeneous systems, the subject of focus here, is rather different: the onset and formation of a condensate in an infinite system is associated with the spontaneous breaking of translational invariance. Also, unlike the traditional equilibrium Bose gas in a box, this real-space condensation in nonequilibrium mass transport models can occur *even in one dimension*.

The purpose of these lectures is to understand the phenomenon of real-space condensation in homogeneous systems

within the context of simple one dimensional mass transport models. The main questions we will be addressing are threefold: (i) When does the condensation happen—i.e. to find the criterion for condensation (ii) How does the condensation happen—i.e., to unfold the mathematical mechanism behind such a transition if it happens and (iii) What is the nature of the condensate—e.g., to compute the distribution of mass or the number of particles in the condensate.

The article is organized as follows. In Section II we will discuss three simple and well studied lattice models of stochastic mass transport. In Section III, we will consider a generalized mass transport model that includes the previous three models as special cases and investigate its steady state. In particular, we will study in detail steady states that are factorisable. The necessary and sufficient conditions for such factorisable property will be discussed. Thanks to this factorisable property, a detailed analytical study of the condensation is possible for such steady states which will be illustrated in Section IV. In Section V we will illustrate how various results associated with the condensation transition in factorisable steady states can be simply understood in terms of sums and extremes of independent and identically distributed (i.i.d) random variables. Finally we will conclude in Section VI with a summary and other possible generalizations/issues associated with the real-space condensation.

II. THREE SIMPLE MASS TRANSPORT MODELS

A. Zero Range Process

The Zero Range Process (ZRP), introduced by Spitzer [12], is perhaps one of the simplest analytically solvable model of mass/particle transport that exhibits a real-space condensation in certain range of its parameters—for a review see [13]. ZRP is defined on a lattice with periodic boundary conditions. For simplicity, we will consider a 1-d lattice with L sites, the generalization to higher dimensions is straightforward. On each site of the lattice at any instant of time rests a number of particles, say m_i at site i where $m_i \geq 0$ is a nonnegative integer. We can also think of each particle carrying a unit mass, so that m_i represents the total mass at site i . A configuration of the system at any given instant is specified by the masses at all sites $\{m_1, m_2, \dots, m_L\}$. One starts from an arbitrary initial condition with a total mass $M = \sum_i m_i$. The subsequent dynamics conserves this total mass or total particle number, or equivalently the density $\rho = M/L$.

The system evolves via continuous-time stochastic dynamics specified by the following rules:

- In a small time interval dt , a single particle from site i with m_i number of particles is transported to its right neighbour $i + 1$ with probability $U(m_i)dt$ provided $m_i \geq 1$. In terms of mass, this means a single unit of mass is transferred from site i to site $i + 1$ with rate $U(m_i)$.

- Nothing happens with probability $1 - U(m_i)dt$.

Here $U(m)$ is an arbitrary positive function, with the constraint that $U(0) = 0$, since there can not be any transfer of unit mass if the site has no mass at all. Thus in ZRP, the particle or mass transfer rate $U(m)$ depends only on the number of particles/mass m at the departure site prior to the transfer. One can of course generalize easily the ZRP to discrete-time dynamics, with symmetric transfer of particles to both neighbours etc [13]. But here we stick to the asymmetric continuous-time model for simplicity.

As the system evolves under this dynamics, the probability of a configuration $P(m_1, m_2, \dots, m_L, t)$ evolves in time and in the long time limit, $t \rightarrow \infty$, it approaches a time-independent stationary joint distribution of masses $P(m_1, m_2, \dots, m_L)$. This is the basic quantity of interest, since the statistics of all other physical observables in the steady state can, in principle, be computed from this joint distribution. In many such nonequilibrium systems, computing the steady state $P(m_1, m_2, \dots, m_L)$ is, indeed, the first big hurdle [8]. Fortunately, in ZRP, this can be computed explicitly and has a rather simple factorised form [12, 13]

$$P(m_1, m_2, \dots, m_L) = \frac{1}{Z_L(M)} f(m_1) f(m_2) \dots f(m_L) \delta\left(\sum_i m_i - M\right) \quad (1)$$

where the weight function $f(m)$ is related to the transfer rate $U(m)$ via

$$\begin{aligned} f(m) &= \prod_{k=1}^m \frac{1}{U(k)} \quad \text{for } m \geq 1 \\ &= 1 \quad \text{for } m = 0 \end{aligned} \quad (2)$$

The delta function in Eq. (1) specifies the conserved total mass M and $Z_L(M)$ is just a normalization factor that ensures that the total probability is unity and satisfies a simple recursion relation

$$Z_L(M) = \sum_{m_i} \prod_{i=1}^L f(m_i) \delta\left(\sum_i m_i - M\right) = \sum_{m=0}^M f(m) Z_{L-1}(M - m). \quad (3)$$

To prove the result in Eq. (1) one simply writes down the Master equation for the evolution of the probability in the configuration space and then verifies [13] that the stationary solution of this Master equation is indeed given by (1).

Finally, the single site mass distribution $p(m)$, defined as the probability that any site has mass m in the steady state, is just the marginal obtained from the joint distribution

$$p(m) = \sum_{m_2, m_3, \dots, m_L} P(m, m_2, m_3, \dots, m_L) = f(m) \frac{Z_{L-1}(M - m)}{Z_L(M)}. \quad (4)$$

Note that $p(m)$ implicitly depends on L but this L dependence has been suppressed for notational simplicity. This single site mass distribution is important as any signature of the existence of a condensate will definitely show up in the explicit form of $p(m)$.

Evidently the steady state $p(m)$ depends on the transfer rate $U(m)$ through the weight function $f(m)$ in Eq. (2). Not all choices of $U(m)$ lead to a steady state with a condensation transition. Indeed, one may ask what choices of $U(m)$ may lead to a condensation transition. An example of such a choice is given by $U(m) \propto (1 + \gamma/m)$ for large m , which leads to, using Eq. (2), a power law weight function, $f(m) \sim m^{-\gamma}$ for large m . In this case, it was shown [2, 13] that for $\gamma > 2$, the system undergoes a condensation transition as one increases the density ρ through a critical value $\rho_c = 1/(\gamma - 2)$. The condensation transition shows up in $p(m)$ in the thermodynamic limit, which has different forms for $\rho < \rho_c$, $\rho = \rho_c$ and $\rho > \rho_c$ [13]

$$\begin{aligned} p(m) &\sim \frac{1}{m^\gamma} \exp[-m/m^*] \quad \text{for } \rho < \rho_c \\ &\sim \frac{1}{m^\gamma} \quad \text{for } \rho = \rho_c \\ &\sim \frac{1}{m^\gamma} + \text{"condensate"} \quad \text{for } \rho > \rho_c \end{aligned} \quad (5)$$

Thus for $\rho < \rho_c$, the single site mass distribution decays exponentially with a characteristic mass m^* that diverges as $\rho \rightarrow \rho_c$ from below, has a power law form exactly at $\rho = \rho_c$ and for $\rho > \rho_c$, while the power-law form remains unchanged, all the additional mass $(\rho - \rho_c)L$ condenses onto a single site which shows up as a bump in $p(m)$ at the tail of the power law form (see Fig. (3)). The term “condensate” in Eq. (5) refers to this additional bump. Physically this means that a single condensate coexists with a background critical fluid for $\rho > \rho_c$. This change of behavior of $p(m)$ as one increases ρ through ρ_c is a prototype signature of the real-space condensation and one finds this behavior in various other stochastic mass transport models that will be discussed below. In addition, many details of the condensation phenomena in ZRP also follow as special cases of the more general mass transport model defined in Section III.

Before ending this subsection, it is useful to point out that there have been several other issues and studies on ZRP and related models that are not covered here. The interested readers may consult the reviews [13, 14].

B. Symmetric Chipping Model

Here we discuss another simple one dimensional mass transport model that also exhibits a condensation phase transition in its steady state. As in ZRP, this model is also defined on a lattice with periodic boundary conditions where each site i carries an integer mass $m_i \geq 0$ [1]. A non-lattice mean-field version of the model was studied in Ref. [15]. The system evolves via the continuous-time dynamics defined by the following rules [1, 16]:

- *diffusion and aggregation*: in a small time interval dt , the entire mass m_i from site i moves either to its right neighbour ($i + 1$) with probability $dt/2$ or to its left neighbour ($i - 1$) with probability $dt/2$.
- *chipping*: in the same interval dt , only one unit of mass chips off site i with mass m_i (provided $m_i \geq 1$) to either its right neighbour with probability $w dt/2$ or to its left neighbour with probability $w dt/2$.
- With probability $1 - (1 + w) dt$ nothing happens.

Once again the total mass $M = \rho L$ is conserved by the dynamics. The model thus has two parameters ρ (density) and w (the ratio of the chipping to the diffusion rate). At long times, the system evolves into a steady state where the single site mass distribution $p(m)$, for large L , exhibits a condensation phase transition at a critical density [1], $\rho_c(w) = \sqrt{w+1} - 1$. Remarkably, this equation of state $\rho_c(w) = \sqrt{w+1} - 1$ turns out to be exact in all dimensions [17] and is thus ‘superuniversal’. For $\rho < \rho_c(w)$, the mass is homogeneously distributed in the system with a mass distribution that has an exponential tail for large mass. At $\rho = \rho_c(w)$, the mass distribution decays as a power law and for $\rho > \rho_c$, a condensate forms on a single site that carries the additional macroscopic mass $(\rho - \rho_c)L$ and coexists with a critical background fluid [1]

$$\begin{aligned} p(m) &\sim \exp[-m/m^*] \quad \text{for } \rho < \rho_c(w) \\ &\sim \frac{1}{m^\tau} \quad \text{for } \rho = \rho_c(w) \\ &\sim \frac{1}{m^\tau} + \text{“condensate”} \quad \text{for } \rho > \rho_c \end{aligned} \quad (6)$$

where the exponent $\tau = 5/2$ within the mean field theory [1] and is conjectured to have the same mean field value even in one dimension [17].

Note that unlike ZRP, the exact joint distribution of masses $P(m_1, m_2, \dots, m_L)$ in the steady state is not known for the symmetric chipping model. In fact, it is believed [17] that $P(m_1, m_2, \dots, m_L)$ does not have a simple product measure (factorisable) form as in ZRP in Eq. (1). Another important difference is that in ZRP, the condensation transition happens both for asymmetric as well as symmetric transfer of masses to the neighbours, as long as one chooses the rate $U(m)$ appropriately. In contrast, for the chipping model, a true condensation transition happens in the thermodynamic limit only for the symmetric transfer of masses. For the asymmetric transfer of masses (say only to the right neighbour), the condensed phase disappears in the thermodynamic limit even though for finite L one does see a vestige of condensation transition [18]. However, a generalization that includes both the chipping model and ZRP as special cases does appear to have a condensation transition even with asymmetric hopping [19]. Finally, when the diffusion rate depends on the mass of the departure site in the chipping model in a certain manner, the condensation transition disappears [20, 21].

This simple chipping model with aggregation and fragmentation rules have been useful in various experimental contexts such as in the growth of palladium nanoparticles [22]. Besides, the possibility of such a condensation phase transition driven by the aggregation mechanism has been discussed in a system of Au sputtered by swift heavy ions [23]. Finally, the chipping model and its various generalizations have also been studied in the context of traffic [24], finance [25] and networks [26].

C. Asymmetric Random Average Process

Another simple mass transport model that has been studied extensively [27, 28, 29, 30] is the asymmetric random average process (ARAP). As in the previous two models, ARAP is defined on a one dimensional lattice with periodic boundary conditions. However, in contrast to ZRP and the chipping model, here the mass m_i at each site i is assumed to be a continuous positive variable. The model has been studied for both continuous-time as well as discrete-time dynamics [27, 28]. In the continuous-time version, the microscopic evolution rules are [27, 28]:

- In a small time interval dt , a random fraction $r_i m_i$ of the mass m_i at site i is transported to the right neighbour ($i+1$) with probability dt , where $r_i \in [0, 1]$ is a random number chosen, independently for each site i , from a uniform distribution over $[0, 1]$.
- With probability $1 - dt$, nothing happens.

The dynamics evidently conserves the total mass $M = \rho L$. At long times, the system reaches a steady state. Once again, the joint distribution of masses $P(m_1, m_2, \dots, m_L)$ in the steady state does not have a factorised product measure form as in ZRP.

How does the single site mass distribution $p(m)$ look like in the large L limit? First important point one notices here is that the density ρ obviously sets the overall mass scale in this model. In other words, the mass distribution $p(m, \rho)$ for any given ρ must have an exact scaling form

$$p(m, \rho) = \frac{1}{\rho} F\left(\frac{m}{\rho}\right) \quad (7)$$

where the scaling function $F(x)$ must satisfy conditions

$$\int_0^\infty F(x)dx = 1; \quad \int_0^\infty x F(x) dx = 1. \quad (8)$$

The first condition follows from normalization, $\int p(m, \rho)dm = 1$ and the second from the mass conservation, $\int m p(m, \rho) dm = \rho$. Since the dynamics involves transferring a uniform fraction of mass from one site to its neighbour, the scaling in Eq. (7) is preserved by the dynamics. This is in contrast to ZRP or the chipping model, where one chips a single unit of mass from one site to its neighbour and thereby the dynamics introduces a separate mass scale (unit mass), in addition to the overall density ρ .

The scaling function $F(x)$ for ARAP has been computed within the mean field theory [27, 28]

$$F(x) = \frac{1}{\sqrt{2\pi x}} e^{-x/2} \quad (9)$$

and this mean field result is remarkably close to the numerical results in one dimension, even though one can prove rigorously [28] that the joint distribution of masses do not factorise. In contrast, for ARAP defined with a parallel discrete-time dynamics (where all sites are updated simultaneously), it has been proved [27, 28] that the joint distribution of masses factorise as in ZRP and the scaling function $F(x)$ for the single site mass distribution can be computed exactly, $F(x) = 4x e^{-2x}$. The steady state of the discrete-time ARAP is also related to the steady state of the so called q -model of force fluctuations in granular materials [31]

What about condensation? In ARAP, one does not find a condensation transition. This is of course expected since the density ρ just sets the mass scale and one does not expect to see a change of behavior in the mass distribution upon increasing ρ , apart from a trivial rescaling of the mass at all sites by a constant factor ρ . However, one can induce a condensation transition in ARAP by inducing an additional mass scale, e.g., by imposing a maximum threshold on the amount of mass that may be transferred from a site to its neighbour [30].

III. A GENERALIZED MASS TRANSPORT MODEL

Let us reflect for a moment what we have learnt so far from the three models discussed above. It is clear that the dynamics of mass transport often, though not always, may lead to a steady state that exhibits real-space condensation. For example, the ZRP and the symmetric chipping model exhibit real-space condensation, but not the ARAP. Also, we note that some of these models such as ZRP have a simple factorisable steady state. But *factorisability of the steady state is clearly not a necessary condition for a system to exhibit real-space condensation*, as we have learnt, e.g., from the study of the symmetric chipping model where the steady state is not factorisable. The factorisability, if present, of course helps the mathematical analysis.

So, a natural question is: given a set of microscopic mass transport rules, what are the necessary and sufficient conditions that they may lead to a steady state that exhibits real-space condensation? For example, from the study of the three models above it seems that in order to have a condensation one needs to introduce via the dynamics a different mass scale, in addition to the density, such as the chipping of a single unit of mass in ZRP and the symmetric chipping model, or via introducing a maximum cap on the mass to be transferred in ARAP. If there is only one overall mass scale (density) that is preserved by the dynamics as in the usual ARAP, one does not expect to see a phase transition in the mass distribution as one changes the density.

This question about finding the conditions for real-space condensation in a generic mass transport model seems too general and is perhaps difficult to answer. Instead, one useful strategy is to restrict ourselves to a special class of mass transport models that have a factorisable steady state and then ask for the criterion, mechanism and nature of the real-space condensation phenomenon within this restricted class of mass transport models, which includes ZRP as a special class. This strategy has been demonstrated to work rather successfully in a recent series of papers [32, 33, 34, 35, 36] and a fairly good understanding of the real-space condensation phenomenon has been developed within this restricted class of mass transport models. This is what we will briefly discuss in this section.

A Generalized Mass Transport Model: One can include all the three models discussed in Section II in a more generalized mass transport model [32]. For simplicity we define the model here on a one dimensional ring of L sites with asymmetric transfer rules, but it can be generalized in a straightforward manner on arbitrary graphs and arbitrary transfer rules. Similar mass transport models with open boundaries as well as dissipation at each site have also been studied [37], though here we restrict ourselves to periodic boundary conditions and non-dissipative dynamics that preserve the total mass. On each site of the ring there is a scalar continuous mass m_i . At any given time t one chooses a mass $0 \leq \mu_i \leq m_i$ independently at each site from a probability distribution $\phi(\mu_i|m_i)$, normalized such that

$\int_0^m \phi(\mu|m) d\mu = 1$. In the time interval $[t, t + dt]$, the mass μ_i is transferred from site i to site $i + 1$, simultaneously for all sites i (see Fig. (1)). In a ring geometry, one identifies the site $(L + 1)$ with the site 1. Thus, after this transfer, the new masses at times $t + dt$ are given by [32]

$$m_i(t + dt) = m_i(t) - \mu_i(t) + \mu_{i-1}(t) \quad (10)$$

where the second term on the right hand side denotes the mass that has left site i and the third term denotes the mass that came to site i from site $(i - 1)$. The function $\phi(\mu|m)$ that specifies the distribution of the stochastic mass to be

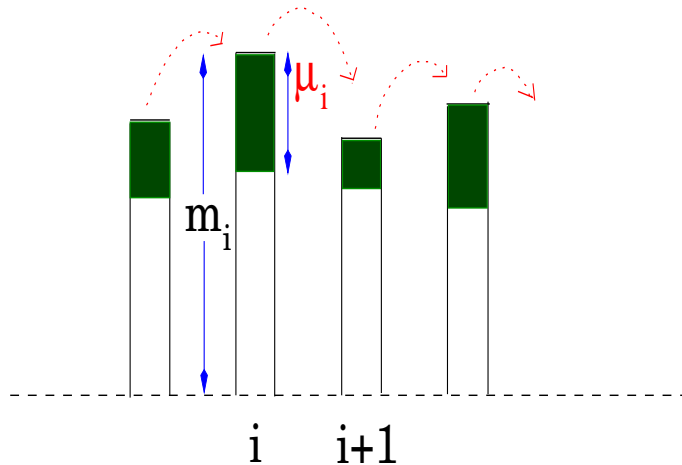


FIG. 1: Generalized mass transport model where a random mass μ_i is transferred from site i with mass m_i to site $i + 1$.

transferred from any given site will be called the ‘chipping kernel’. Here we take a homogeneous chipping kernel $\phi(\mu|m)$ which does not depend on the site index. Note that the model above has been defined with parallel dynamics where all sites are updated simultaneously. Of course, by chossing $dt \rightarrow 0$, one can recover the continuous-time random sequential dynamics where the probability that two sites will be updated simultaneously is very small $\sim O((dt)^2)$. Thus the parallel dynamics includes the continuous-time (random sequential) dynamics as a special case. Note that for random sequential dynamics $\phi(\mu|m)$ must generically be of the form

$$\phi(\mu|m) = \alpha(\mu|m)dt + \left[1 - dt \int_0^m \alpha(\mu'|m)d\mu' \right] \delta(\mu) \quad (11)$$

where $\alpha(\mu|m)$ denotes the *rate* at which a mass μ leaves a site with mass m and the second term denotes the probability that no mass leaves the site. The form in Eq. (11) is designed so that it automatically satisfies the normalization condition: $\int_0^m \phi(\mu|m) d\mu = 1$.

This model with a general chipping kernel $\phi(\mu|m)$ includes the previously discussed ZRP, chipping model and ARAP as special cases [32]. Since we introduced these models in the previous section in continuous time, we will consider here the generalized model with chipping kernel of the form in Eq. (11) with a general chipping rate $\alpha(\mu|m)$. But of course one can consider a more general $\phi(\mu|m)$ with parallel dynamics that includes the continuous-time dynamics as a special case. Let us consider the three examples:

(i) As a first example, we see that ZRP is recovered if in Eq. (11) we choose for $0 \leq \mu \leq m$

$$\alpha(\mu|m) = U(m)\delta(\mu - 1) \quad (12)$$

Note that $U(m)$ is zero if $m < 1$.

(ii) Similarly, the asymmetric chipping model is recovered if we choose

$$\alpha(\mu|m) = w\delta(\mu - 1) + \delta(\mu - m) \quad (13)$$

where the first term refers to the event of a transfer of single unit of mass with rate w , the second term refers to the transfer of the full mass m with rate 1.

(iii) Finally, one recovers ARAP by choosing

$$\alpha(\mu|m) = \frac{1}{m} \quad (14)$$

for all $0 \leq \mu \leq m$ corresponding to the transfer of a fraction of mass that is chosen uniformly in $[0, 1]$ leading to a uniform rate $\alpha(\mu|m)$ independent of μ .

By appropriately choosing the chipping kernel $\phi(\mu|m)$, or equivalently the rate $\alpha(\mu|m)$ for continuous-time dynamics, one can construct a whole class of mass transport models thus justifying the name ‘generalized mass transport model’.

Given a general chipping kernel $\phi(\mu|m)$, or equivalently the chipping rate $\alpha(\mu|m)$ for continuous-time dynamics, one can ask two important questions: (i) What is the steady state joint mass distribution $P(m_1, m_2, \dots, m_L)$? (ii) Which types of $\phi(\mu|m)$, or equivalently $\alpha(\mu|m)$ for continuous-time dynamics, lead to a real-space condensation transition in the steady state? As discussed earlier, answers to either of these questions are hard to provide for a general chipping kernel $\phi(\mu|m)$ (or chipping rate $\alpha(\mu|m)$). However, let us now restrict ourselves only to those chipping kernels $\phi(\mu|m)$ (or $\alpha(\mu|m)$) that lead to a factorised steady state distribution of the form

$$P(m_1, m_2, \dots, m_L) = \frac{1}{Z_L(M)} f(m_1) f(m_2) \dots f(m_L) \delta\left(\sum_i m_i - M\right) \quad (15)$$

where the partition function $Z_L(M)$ is just a normalization constant. This then leads us to the restricted mass transport model with factorisable steady state and we will address the questions regarding real-space condensation within this restricted class. The answers to these questions turn out to be easier for this restricted class since one can make use of the exact form of the steady state joint mass distribution (15).

A Restricted Mass Transport Model: Here we restrict ourselves only to those chipping kernels that lead to a factorisable steady state (15). Let us first investigate the question: given $\phi(\mu|m)$ (or equivalently $\alpha(\mu|m)$ for continuous-time dynamics), what is the necessary and sufficient condition on $\phi(\mu|m)$ that leads to a factorisable steady state as in Eq. (15) and if it happens, what is the exact form of the weight function $f(m)$ in terms of $\phi(\mu|m)$? Fortunately, answers to both questions can be obtained exactly which we state below without giving the details of the proof (see Ref. ([32]) for details). The necessary and sufficient condition for factorisability is that $\phi(\mu|m)$ must be of the form [32]

$$\phi(\mu|m) = \frac{v(\mu) w(m - \mu)}{\int_0^m v(y) w(m - y) dy} \quad (16)$$

where $v(x)$ and $w(x)$ are arbitrary positive functions and the denominator is chosen to ensure normalizability, $\int_0^m \phi(\mu|m) d\mu = 1$. In other words, if the chipping kernel $\phi(\mu|m)$ factorises into a function of the mass that leaves the site and a function of the mass that stays on the site, then the steady state is guaranteed to be factorisable as in Eq. (15) with a weight function whose exact form is given by the denominator in Eq. (16)

$$f(m) = \int_0^m v(y) w(m - y) dy. \quad (17)$$

This is the sufficiency condition. On the other hand, this condition can also be proved to be necessary, i.e., given that the steady state is of the form (15) with some $f(m)$, the chipping kernel has to be of the type (16) and $f(m)$ then must have the form (17).

Analogous condition can be found for continuous-time dynamics where $\phi(\mu|m)$ has the form (11) with a chipping rate $\alpha(\mu|m)$. The necessary and sufficient condition stated above for $\phi(\mu|m)$, translates into the following condition on $\alpha(\mu|m)$ [32],

$$\alpha(\mu|m) = y(\mu) \frac{z(m - \mu)}{z(m)} \quad (18)$$

where $y(x)$ and $z(x)$ are two arbitrary positive functions. Note that $\alpha(\mu|m)$ is a rate (and not a probability) and hence there is no normalization condition here to be satisfied. If the rate $\alpha(\mu|m)$ has the form (18) then we are guaranteed to reach a factorisable steady state (15) with a simple weight function [32]

$$f(m) = z(m). \quad (19)$$

As an example, it is easy to verify that the chipping rate in ZRP (12) can indeed be written in the form in Eq. (18) by choosing $y(\mu) = \delta(\mu - 1)$ and $z(m) = \prod_{k=1}^m \frac{1}{U(k)}$ for $m \geq 1$, $z(0) = 1$ and $z(m < 0) = 0$. Thus, ZRP with sequential dynamics is guaranteed to have a factorisable steady state (15) with the weight function, $f(m) = z(m) = \prod_{k=1}^m \frac{1}{U(k)}$ for $m \geq 1$ and $f(0) = z(0) = 1$. In contrast, both for asymmetric chipping model and the ARAP with chipping rates given respectively in (13) and (14) can not be written in the form (18) with some choice of nonnegative functions $y(x)$ and $z(x)$, proving that neither of these two models has a factorisable steady state.

One can ask several other interesting related questions. For example, suppose we are given a chipping kernel $\phi(\mu|m)$ and we want to know if it has a factorisable steady state or not. This amounts to an explicit search for suitable nonnegative functions $v(x)$ and $w(x)$ such that the kernel $\phi(\mu|m)$ can be written as in Eq. (16). This is often laborious. Can one devise a simple test which will allow us to do this search quickly just by looking at the functional form of $\phi(\mu|m)$? It turns out that indeed one can devise such a simple test which is stated as follows [33]: Given $\phi(\mu|m)$, first set $m = \mu + \sigma$ and compute the following two derivatives

$$q(\mu, \sigma) = \partial_\mu \partial_\sigma \log [\phi(\mu|\mu + \sigma)] \quad (20)$$

which, in general, is a function of both variables μ and σ . The test devised in Ref. [33] states that a given $\phi(\mu|m)$ will lead to a factorisable steady state iff this function $q(\mu, \sigma)$ in Eq. (20) is only a function of the single variable $\mu + \sigma$, i.e.,

$$q(\mu, \sigma) = h(\mu + \sigma) \quad (21)$$

and in that case the weight function $f(m)$ in the factorisable steady state (15) is given explicitly by

$$f(m) = \exp \left[- \int^m dx \int^x dy h(y) \right]. \quad (22)$$

In the discussion above, we have focused only on the ring geometry with asymmetric transfer of mass. Some of these results can be partially generalized to higher dimensions and even to arbitrary graphs [36, 38] and also to transport models with more than one species [39] of scalar variables, such as mass and energy for instance.

IV. CONDENSATION IN MASS TRANSPORT MODELS WITH FACTORISABLE STEADY STATE

In this section we discuss issues related to condensation within the restricted class of mass transport models that have a special steady state—namely a factorisable joint distribution (15) with a suitable weight function $f(m)$. We note that some aspects of the condensation transition in such a factorisable steady state, notably properties in the fluid state, was first studied in the context of the Backgammon model [40] without recourse to the dynamics that gives rise to such a factorisable steady state. A more complete analysis including the study of the properties of the condensed phase was undertaken in Refs. [34, 35] which will be summarized in this section.

There are three main issues here: (i) *criterion*: what kind of weight functions $f(m)$ lead to a condensation transition (ii) *mechanism*: what is the mechanism of the condensation transition when there is one and (iii) *nature*: what is the nature of the condensate, e.g., what is the statistics of the mass in the condensate in the condensed phase? All these questions can be answered in detail for factorisable steady states. We briefly mention the main results here, the details can be found in Refs. [34, 35].

Criterion: The factorisation property (15) allows one to find the criterion for a condensation transition rather easily by working in the grand canonical ensemble (GCE). Within GCE framework, one introduces a fugacity $\exp[-s m]$ where s is the negative of the chemical potential associated with each site. This is just equivalent to taking the Laplace transform of Eq. (15) with respect to the total mass M (with s being the Laplace variable), which replaces the delta function by $\exp[-s(m_1 + m_2 + \dots m_L)]$. Then s is chosen such that the constraint $M = \sum m_i$ is satisfied on an average. Given that each site now has a mass distribution $p(m) = f(m) \exp[-s m]$ (upto a normalization constant), the equation that fixes the value of s for a given $M = \rho L$ is simply

$$\rho = \rho(s) \equiv \frac{\int_0^\infty m f(m) e^{-sm} dm}{\int_0^\infty f(m) e^{-sm} dm}. \quad (23)$$

The criterion for condensation can be derived easily by analysing the function $\rho(s)$ defined in Eq. (23). If for a given ρ , one finds a solution to this equation $s = s^*$ such that the single site mass distribution is normalizable, i.e., $\int p(m) dm = \int f(m) \exp[-s^* m] dm$ is finite, then there is no condensation in the sense that for all values of ρ , the single site mass distribution has an exponential tail and there is not one special site that needs to accomodate extra mass. On the other hand, it may be that for certain $f(m)$'s, as one increases ρ , there may be a critical value ρ_c below which one finds a good solution s to Eq. (23), but such a solution ceases to exist for $\rho > \rho_c$. This will then signal the onset of a condensation because for $\rho > \rho_c$, the system needs to break up into two parts: (a) a critical background fluid part consisting of $(L - 1)$ sites at each of which the average density is critical ρ_c and (b) a single condensate site which accomodates the additional mass $(\rho - \rho_c)L$.

As an example, let us consider $f(m)$ that decays slower than an exponential, but faster than $1/m^2$ for large m . Since $f(m)$ decays slower than an exponential, in order that the single site mass distribution $p(m) = f(m) e^{-s^* m}$ is normalizable (i.e., $\int p(m) dm = 1$), the possible solution s^* of Eq. (23) can not be negative. Thus the lowest possible solution is $s^* = 0$. Now as $s \rightarrow 0$, the function $\rho(s)$ in (23) approaches a critical value,

$$\rho_c = \rho(s \rightarrow 0) = \frac{\int_0^\infty m f(m) dm}{\int_0^\infty f(m) dm} \quad (24)$$

which is finite since $f(m)$ decays faster than $1/m^2$ for large m . Thus as long as $\rho < \rho_c$, by solving (23) one will get a positive solution s^* and hence no condensation. As $\rho \rightarrow \rho_c$ from below, $s^* \rightarrow 0$ from above. But for $\rho > \rho_c$, there is no positive solution s^* to (23), which signals the onset of a condensation transition.

A detailed analysis of Eq. (23) shows [35] that in order to have condensation, the weight function $f(m)$ must have a large m tail that lies above an exponential but below $1/m^2$, i.e., $\exp[-cm] < f(m) < 1/m^2$ for large m with some positive constant $c > 0$. A natural candidate satisfying this criterion is

$$f(m) \simeq A m^{-\gamma} \quad \text{with} \quad \gamma > 2 \quad (25)$$

for large m . Indeed, the ZRP discussed in the previous sections with the choice $U(m) \sim (1 + \gamma/m)$ for large m leads to a weight function $f(m)$ (25) and then condensation happens only for $\gamma > 2$.

Mechanism and Nature: Given an appropriate weight function $f(m)$ such as in (25) that leads to condensation, one can then ask about the mathematical mechanism that drives the condensation. Actually, there is a very simple way to understand this mechanism in terms of sums of random variables [35] which we will discuss in the next section. For now, we notice that in an infinite system, where GCE is appropriate, the single site mass distribution $p(m)$ has the form $p(m) = f(m) \exp[-sm]$ with an appropriate s which is the solution of Eq. (23) as long as $\rho < \rho_c$. For $\rho > \rho_c$, there is no solution to Eq. (23). In fact, for $\rho > \rho_c$, the value of s sticks to its critical value s_c and the GCE framework is no longer valid. To understand how the condensation manifests itself in the single site mass distribution, one has to study a system with a finite size L and work in the canonical ensemble with a strict delta function constraint as in Eq. (15).

In a finite system of size L , the single site mass distribution $p(m)$ can be obtained by integrating the joint distribution (15) over the masses at all sites except one where the mass is fixed at m . It is easy to see from Eq. (15) that

$$p(m) = \int P(m, m_1, m_2, \dots, m_L) dm_2 dm_3 \dots dm_L = f(m) \frac{Z_{L-1}(M-m)}{Z_L(m)} \quad (26)$$

where the partition function $Z_L(M)$

$$Z_L(M) = \int f(m_1) f(m_2) f(m_L) \delta\left(\sum_i m_i - M\right) dm_1 dm_2 \dots dm_L. \quad (27)$$

Taking Laplace transform with respect to M , one gets

$$\int_0^\infty Z_L(M) e^{-sM} dM = \left[\int_0^\infty f(m) e^{-sm} dm \right]^L \quad (28)$$

which can be formally inverted using the Bromwich formula

$$Z_L(M) = \int_{s_0 - i\infty}^{s_0 + i\infty} \frac{ds}{2\pi i} \exp[L(\ln g(s) + \rho s)] \quad (29)$$

where we have used $M = \rho L$, the integral runs along the imaginary axis ($s_0 + i y$) in the complex s plane to the right of all singularities of the integrand and

$$g(s) \equiv \int_0^\infty f(m) e^{-s m} dm. \quad (30)$$

One can write a similar integral representation of the numerator $Z_L(M - m)$ in Eq. (26). Next one analyses $Z_L(M)$ and $Z_L(M - m)$ using the method of steepest decent in the large L limit.

As long as there is a saddle point solution to Eq. (29), say at $s = s^*$, we see immediately from Eq. (26) that the single site mass distribution for large L has the form, $p(m) \sim f(m) \exp[-s^* m]$, i.e., one recovers the GCE result. Thus the GCE approach is valid as long as there is a saddle point solution s^* . As one increases ρ , the saddle s^* starts moving towards 0 in the complex s plane and when ρ hits ρ_c , $s^* \rightarrow 0$. For $\rho > \rho_c$, there is no saddle point and one has to analyse the Bromwich integrals by correctly choosing the contour to evaluate $p(m)$ for $\rho > \rho_c$. This was done in details in Ref. [35]. We omit the details here and mention the main results for $Z_L(M)$ in Eq. (29) and subsequently for $p(m)$ in Eq. (26), when the weight function $f(m)$ is chosen to be of the power law form (25).

If we normalize $f(m)$ such that $\int_0^\infty f(m) dm = 1$, the partition function in Eq. (29) can be interpreted as the probability that the sum of L i.i.d variables, each drawn from a distribution $f(m)$, is M (see Section V also). Analysing the Bromwich integral (29) for large L , using the small s behavior of $g(s)$ in Eq. (30), one finds [35] that the asymptotic behavior of the distribution $Z_L(M)$ is different for $2 < \gamma \leq 3$ and for $\gamma > 3$.

$2 < \gamma \leq 3$: In this regime, one finds the following scaling behavior of $Z_L(M)$

$$Z_L(M) \simeq \frac{1}{L^{1/(\gamma-1)}} V_\gamma \left[\frac{\rho_c L - M}{L^{1/(\gamma-1)}} \right] \quad (31)$$

where $\rho_c = \mu_1 = \int_0^\infty m f(m) dm$ is the first moment and the function $V_\gamma(z)$ is given explicitly by [35]

$$V_\gamma(z) = \frac{1}{\pi} \int_0^\infty dy e^{-c_3 y^{\gamma-1}} \cos [b \cos(\pi\gamma/2) y^{\gamma-1} + yz]. \quad (32)$$

Here $c_3 = -b \sin(\pi\gamma/2) > 0$ and $b = A \Gamma(1 - \gamma)$ for $2 < \gamma < 3$ with A being the amplitude in (25). The precise asymptotic tails of this scaling function can be computed [35]

$$V_\gamma(z) \simeq A |z|^{-\gamma} \quad \text{as } z \rightarrow -\infty \quad (33)$$

$$= c_0 \quad \text{at } z = 0 \quad (34)$$

$$\simeq c_1 z^{(3-\gamma)/2(\gamma-2)} e^{-c_2 z^{(\gamma-1)/(\gamma-2)}} \quad \text{as } z \rightarrow \infty \quad (35)$$

where c_0 , c_1 and c_2 are known constants [35]. Thus the function is manifestly non-gaussian.

$\gamma > 3$: In this regime, the partition function $Z_L(M)$ has a gaussian peak

$$Z_L(M) \simeq \frac{1}{\sqrt{2\pi\Delta^2 L}} e^{-(M-\rho_c L)^2/2\Delta^2 L} \quad \text{for } |M - \rho_c L| \ll O(L^{2/3}) \quad (36)$$

where $\Delta^2 = \mu_2 - \mu_1^2$ with $\mu_k = \int_0^\infty m^k f(m) dm$ being the k -th moment. But far to the left of the peak, $Z_L(M)$ has a power law decay [35].

So, how does the single site mass distribution $p(m)$ in Eq. (26) look like? We have to use the result for the partition function derived above in Eq. (26). We find different behaviors of $p(m)$ in different regions of the $(\rho - \gamma)$ plane. For $\gamma > 2$, there is a critical curve $\rho_c(\gamma)$ in the $(\rho - \gamma)$ plane that separates a fluid phase (for $\rho < \rho_c(\gamma)$) from a condensed phase (for $\rho > \rho_c(\gamma)$). In the fluid phase the mass distribution decays exponentially for large m , $p(m) \sim \exp[-m/m^*]$ where the characteristic mass m^* increases with increasing density and diverges as the density approaches its critical value ρ_c from below. At $\rho = \rho_c$ the distribution decays as a power law, $p(m) \sim m^{-\gamma}$ for large m . For $\rho > \rho_c$, the distribution, in addition to the power law decaying part, develops an additional bump, representing the condensate, centred around the ‘‘excess’’ mass:

$$M_{ex} \equiv M - \rho_c L. \quad (37)$$

Furthermore, by our analysis within the canonical ensemble, we show that even inside the condensed phase ($\rho > \rho_c(\gamma)$), there are two types of behaviors of the condensate depending on the value of γ . For $2 < \gamma < 3$, the condensate is

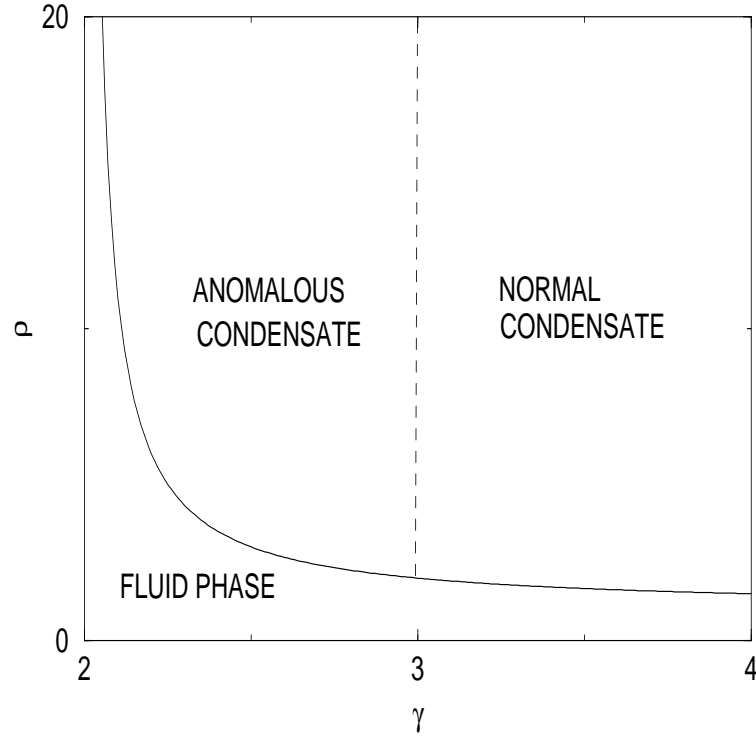


FIG. 2: Schematic phase diagram in the ρ - γ plane.

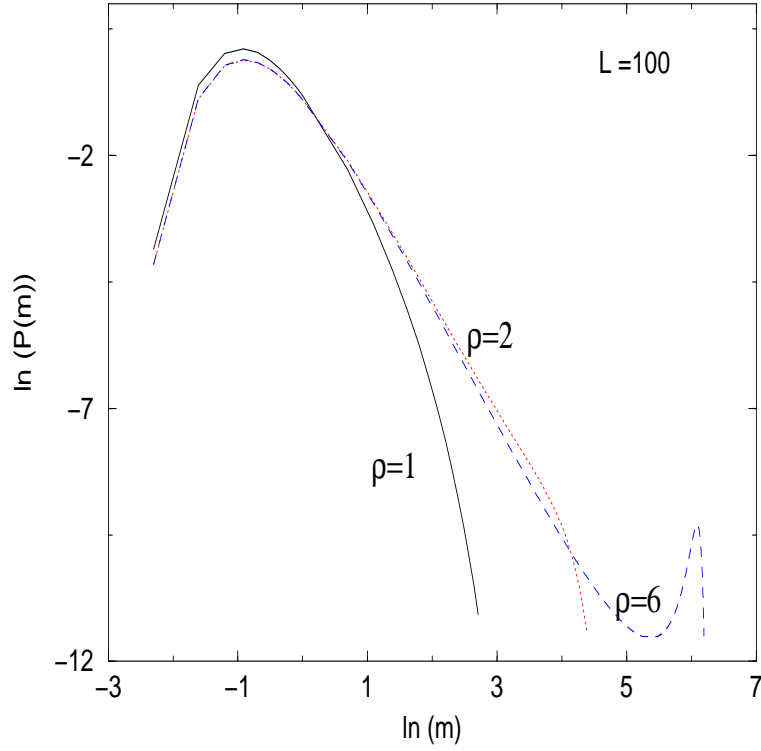


FIG. 3: The exact single-site mass distribution $p(m)$ plotted for a particular choice of $f(m)$ with $\gamma = 5/2$ and $\rho_c = 2$, and system size $L = 100$: full line $\rho = 1$ (subcritical: fluid phase); dotted line $\rho = 2$ (critical); dashed line $\rho = 6$ (supercritical: condensed phase). the condensate bump, $p_{\text{cond}}(m)$, is evident in the supercritical phase.

characterized by anomalous non-gaussian fluctuations whereas for $\gamma > 3$, the condensate has gaussian fluctuations. This leads to a rich phase diagram in the $(\rho - \gamma)$ plane, a schematic picture of which is presented in Fig. (2).

Detailed form of $p(m)$ for $\rho < \rho_c$ (fluid phase), $\rho > \rho_c$ (condensed phase) and $\rho = \rho_c$ (critical point) are summarized below (see Fig. (3) also).

Fluid phase $\rho < \rho_c$: In this case one finds

$$p(m) \sim f(m) e^{-m/m^*} \quad \text{for } 1 \ll m \ll M \quad (38)$$

where the characteristic mass m^* diverges ρ approaches ρ_c from below as $(\rho - \rho_c)^{-1}$ for $\gamma > 3$ and $(\rho - \rho_c)^{-1/(\gamma-2)}$ for $2 < \gamma < 3$.

Condensed Phase $\rho > \rho_c$: In this case one finds

$$p(m) \simeq f(m) \quad \text{for } 1 \ll m \ll O(L) \quad (39)$$

$$p(m) \simeq f(m) \frac{1}{(1-x)^\gamma} \quad \text{for } m = xM_{ex} \quad \text{where } 0 < x < 1 \quad (40)$$

$$p(m) \sim p_{\text{cond}}(m) \quad \text{for } m \sim M_{ex} \quad (41)$$

Here p_{cond} is the piece of $p(m)$ which describes the condensate bump (see Fig. (3): Centred on the excess M_{ex} and with integral being equal to $1/L$, it takes on two distinct forms according to whether $\gamma < 3$ or $\gamma > 3$.

For $2 < \gamma < 3$

$$p_{\text{cond}}(m) \simeq L^{-\gamma/(\gamma-1)} V_\gamma \left[\frac{m - M_{ex}}{L^{1/(\gamma-1)}} \right], \quad (42)$$

where the function $V_\gamma(z)$ is given explicitly in (32). Thus clearly the condensate bump has a non-gaussian shape for $2 < \gamma < 3$ and we refer to this as an ‘anomalous’ condensate.

On the other hand, for $\gamma > 3$

$$p_{\text{cond}}(m) \simeq \frac{1}{\sqrt{2\pi\Delta^2 L^3}} e^{-(m-M_{ex})^2/2\Delta^2 L} \quad \text{for } |m - M_{ex}| \ll O(L^{2/3}). \quad (43)$$

i.e. $p_{\text{cond}}(m)$ is gaussian on the scale $|m - M_{ex}| \ll O(L^{2/3})$, but, far to the left of the peak, $p(m)$ decays as a power law.

Critical density $\rho = \rho_c$: In this case one finds that

$$p(m) \propto f(m) V_\gamma \left(m/L^{1/(\gamma-1)} \right), \quad \text{for } 2 < \gamma < 3 \quad (44)$$

$$p(m) \propto f(m) e^{-m^2/2\Delta^2 L} \quad \gamma > 3. \quad (45)$$

where the scaling function $V_\gamma(z)$ is as before. Thus at criticality $p(m)$ decays as a power law $m^{-\gamma}$ for large m which is cut-off by a finite size scaling function and the cut-off mass scales as

$$m_{\text{cut-off}} \sim L^{1/(\gamma-1)} \quad \text{for } 2 < \gamma < 3 \quad (46)$$

$$\sim L^{1/2} \quad \text{for } \gamma > 3. \quad (47)$$

Physical picture: It is useful to summarize the main physical picture that emerges out of this mathematical analysis. We notice from the joint distribution (15) that the masses at each site are ‘almost’ independent random variables each with a power law distribution $f(m)$, except for the global constraint of mass conservation imposed by the delta function which actually makes them ‘correlated’. The system feels this correlation for $\rho < \rho_c$ and $\rho > \rho_c$ in different ways and exactly at the critical point $\rho = \rho_c$ the effect of the constraint is actually the least. For $\rho < \rho_c$, the effective mass distribution at each site acquires an exponential tail, $p(m) \sim f(m) \exp[-s^* m]$ which is induced by the constraint. For $\rho = \rho_c$, $s^* \rightarrow 0$ and $p(m) \sim f(m)$, thus the system does not feel the constraint at all and the masses behave as completely independent random variables each distributed via $f(m)$. But for $\rho > \rho_c$, while $(L-1)$ sites behave as the critical fluid, i.e., as if the mass at each of these $(L-1)$ sites is distributed via $f(m)$, there is one single condensate site which acquires the additional mass $(\rho - \rho_c)L$.

For $\rho > \rho_c$, the resulting non-monotonous shape of the single site mass distribution (with an additional bump) in Fig. (3) can then be understood very easily from this physical picture. Basically, for $\rho > \rho_c$, the total mass M of the system splits into the critical fluid and the condensate part:

$$M = m_{\text{cond}} + M_{\text{fluid}} \quad (48)$$

where m_{cond} denotes the mass at the condensate and the critical background fluid mass

$$M_{\text{fluid}} = \sum_{i=1}^{L-1} m_i \quad (49)$$

is a sum of $(L-1)$ independent random variables (masses) each distributed via $f(m)$. Thus the probability distribution M_{fluid} is given precisely by the partition function $Z_{L-1}(M_{\text{fluid}})$ in Eq. (27). This partition function can be computed explicitly and the results are given in Eqs. (31) and (36). Knowing this partition function, the distribution of the condensate mass m_{cond} can be obtained using Eq. (48) giving

$$\text{Prob}(m_{\text{cond}} = y) = Z_{L-1}(M - y). \quad (50)$$

The overall single site mass distribution for $\rho > \rho_c$ then can be computed as follows: if we choose a site at random, with probability $(L-1)/L$ it belongs to the background fluid and hence its mass distribution is $f(m)$ whereas with probability $1/L$ it will be the condensate site with mass distribution given in Eq. (50). Thus for $\rho > \rho_c$

$$p(m) \approx \frac{(L-1)}{L} f(m) + \frac{1}{L} Z_{L-1}(M - m) \quad (51)$$

The second term is what we referred to before as

$$p_{\text{cond}}(m) = \frac{1}{L} Z_{L-1}(M - m) \quad (52)$$

and it is this piece that describes the bump in Fig. (3) for $\rho > \rho_c$. Its precise asymptotic behavior is detailed in Eqs. (42) and (43) respectively for $2 < \gamma \leq 3$ and $\gamma > 3$.

V. INTERPRETATION AS SUMS AND EXTREMES OF RANDOM VARIABLES

There is a very nice and simple way [35], using sums of random variables, to understand the mechanism of the condensation transition for factorisable steady states (15) with a given weight function $f(m)$ say of the form (25). Let us consider a set of L positive i.i.d random variables $\{m_1, m_2, \dots, m_L\}$ each drawn from a distribution $f(m)$ (we choose $f(m)$ such that it is normalized to unity). Let $M = \sum_{i=1}^L m_i$ be the sum. For instance, M can be interpreted as the position of a random walker after L independent steps of lengths m_1, m_2, \dots, m_L . Then we notice that the partition function $Z_L(M)$ in Eq. (27) can be interpreted as the probability that the walker reaches M in L steps starting from the origin.

How does one interpret condensation in this random walk language? Note from Eq. (24) that for normalized (to unity) $f(m)$, the critical density

$$\rho_c = \mu_1 = \int_0^\infty m f(m) dm \quad (53)$$

is just the mean step length of the random walker's steps. Thus if the final position $M < \rho_c L = \mu_1 L$ (i.e., $\rho = M/L < \rho_c$), we would expect that the typical configuration of the random walker's path would consist of steps each of which is of $\sim O(1)$. But, for $M > \mu_1 L$ (i.e., $\rho > \rho_c$), the ensemble will be dominated by configurations where $(L-1)$ steps are of $\sim O(1)$, but one single big step of $\sim (M - \mu_1(L-1)) \sim (\rho - \rho_c)L$ to compensate for the deficit distance. This single big step is precisely the condensate. Within this interpretation, it also becomes clear that for $f(m)$ of the form (25), there are two possibilities depending on whether the second moment of the step length distribution $\mu_2 = \int_0^\infty m^2 f(m) dm$ is divergent ($2 < \gamma \leq 3$) or finite ($\gamma > 3$). In the former case, the corresponding random walker is a Lévy flight with anomalously large fluctuations that leads to an anomalously large fluctuation in the condensate mass. In the latter case, by virtue of the central limit theorem, one recovers a gaussian fluctuation leading to a gaussian distribution of the condensate mass. This explains the two types of condensate phases in the phase diagram in Fig. (2).

Condensation and Extreme Statistics: Another interesting issue intimately related to the condensation is the associated extreme value statistics—e.g, what is the distribution of the largest mass m_{max} in the system, where

$$m_{\text{max}} = \max(m_1, m_2, \dots, m_L). \quad (54)$$

This is particularly important in the condensed phase where the largest mass is carried by the condensate, at least in models with simple factorised steady states where there is a single condensate. The theory of extreme value statistics

is well developed in cases where one studies the extreme (e.g., the maximum) of a set of i.i.d random variables [41]. In our case, the factorised steady state in Eq. (15) shows that the masses are not completely independent, but are correlated via the global mass conservation constraint explicitly manifest in the delta function in Eq. (15). Without this delta function constraint, with $f(m) \sim m^{-\gamma}$ and $\gamma > 2$, the scaled distribution of the maximal mass would have been Fréchet distribution [41]. However the presence of the constraint induces important correlations that changes the nature of the distribution of the maximal mass.

In Ref. [42], the authors studied rigorously how the typical value of the extremal mass scales with system size in ZRP with $\gamma > 3$. For more general mass transport models with factorised steady states as in Eq. (15), the full distribution of extremal mass was studied recently in Ref. [43]. It was found that in the fluid phase ($\rho < \rho_c$), where the single site masses effectively become uncorrelated but with an additional $\exp[-s^*m]$ factor that comes from the conservation constraint: $p(m) \sim f(m) \exp[-s^*m]$ and hence the maximal mass, in the scaling limit, becomes Gumbel [43]. At the critical point where $s^* = 0$ (i.e., where the constraint is least effective), one recovers the Fréchet distribution. But for $\rho > \rho_c$ the maximal mass distribution is the same as that of the condensate mass, i.e.,

$$m_{\max} = m_{\text{cond}} \quad (55)$$

However, as mentioned in the previous section, the distribution of $m_{\text{cond}} = M - M_{\text{fluid}}$ can be computed via computing the distribution of M_{fluid} as a sum of independent random variables each distributed via $f(m)$ and is given by Eq. (50). Thus,

$$\text{Prob}(m_{\max} = y) \approx Z_{L-1}(M - y) = L p_{\text{cond}}(y) \quad (56)$$

where $p_{\text{cond}}(m)$ is given in Eqs. (42) and (43) respectively for $2 < \gamma < 3$ and $\gamma > 3$. Thus, in the condensed phase, one has a completely new type of extreme value distribution of correlated random variables which is exactly computable [43]. Moreover, it is interesting to note that for $\rho > \rho_c$, the computation of the distribution of the extreme of correlated variables reduces to the calculation of the distribution of sum of independent random variables.

VI. CONCLUSION

In this brief review I discussed recent developments in understanding the physics of the real-space condensation in a class of mass transport models. Here, real-space condensation refers to the phenomenon when, upon increasing the density beyond a critical value, a macroscopically large mass settles onto a single site in real space in the steady state. The system discussed is homogeneous in the sense that the transport rules do not depend on the sites or particles. Thus, in the limit of an infinite system size, the formation of the condensate at one single site actually breaks the translational symmetry in the system spontaneously. The criterion and mechanism of the transition as well as the detailed finite size dependence of the distribution of the condensate mass in the condensed phase was discussed within a restricted class of one dimensional mass transport models that have a factorisable steady state.

There are several directions in which the questions addressed here can be extended, some of which are briefly mentioned below.

Pair factorised steady states: Here we discussed only mass transport models that have a factorised steady state (15). A natural question is whether real-space condensation can happen in other types of steady states that are not simply factorisable as in (15) and if so, (i) are there natural *local* transport rules that lead to such steady states and (ii) does the nature of the condensate change fundamentally from the one with factorisable steady states? Recently, a generalization of Eq. (15), called the pair factorised steady states (PFSS) was introduced in Ref. [44]

$$P(m_1, m_2, \dots, m_L) = \frac{1}{Z_L(M)} \prod_{i=1}^L g(m_i, m_{i+1}) \delta \left(\sum_{i=1}^L m_i - M \right). \quad (57)$$

Thus there is one factor $g(m_i, m_{i+1})$ for each pair of neighbouring sites on a ring of L sites. The transport rules, involving three neighbouring sites, that lead to such steady states were also found [44]. Interestingly, the condensate in this PFSS, for a class of weight functions $g(m, n)$ that are short ranged, was found to spread over a relatively large number of sites $\sim O(L^{1/2})$ [44], in contrast to the condensate that forms over a single site in the usual factorised steady state (15). The average shape of this sub-extensive condensate for a class of weight functions $g(m, n)$ as well as the precise form of the ‘condensate bump’ in the single site mass distribution in the condensed phase were recently computed in a very nice paper [45]. In addition, the transport rules that lead to PFSS on an arbitrary graph were also found recently [46], thus generalizing the one dimensional models with PFSS.

Dynamics: Here we have discussed only static properties associated with the condensation transition. Another interesting issue is the nature of the dynamics in the steady state as well as in the approach to the steady state, in particular in the condensed phase [47, 48, 49, 50, 51]. In a finite system, the condensate forms at a site, then survives there over a long time T_s , then desolves and then forms at another site. For ZRP with $f(m) \sim m^{-\gamma}$ with $\gamma > 2$ and in the stationary state, it was found that while the condensate life-time $T_s \sim (\rho - \rho_c)^{\gamma+1} L^\gamma$ for large L [49], there is another shorter time scale associated with the relocation of the condensate, $T_r \sim (\rho - \rho_c)^2 L^2$ [50]. In addition, the current fluctuations in the steady state show a striking change of behavior [50] as one goes from the fluid phase ($\rho < \rho_c$) to the condensed side ($\rho > \rho_c$). On the fluid side, the current fluctuations shows an interesting oscillating behavior due to the presence of kinematic waves [50], similar to the oscillatory behavior of the variance in the displacement of a tagged particle in 1-d asymmetric exclusion processes [52]. Another interesting dynamical quantity is the power spectra associated with the time series depicting the evolution of the total number of particles over a fixed segment of a ring, studied recently in the context of ZRP [53].

It would be interesting to study the dynamics for the mass transport models in higher dimensions or arbitrary graphs, and also for more generalized steady states such as the PFSS.

Other interesting directions involve studying the condensation phenomena in multispecies models [13, 39], misanthropic process [13], instability of the condensed phase due to nonconserving rates in the chipping model [1, 54] as well as in ZRP [55, 56] and also in ZRP due to quench disordered particle transfer rate [57], ZRP leading to multiple condensates [58], condensation in polydisperse hard spheres [59] etc. Most of these generalizations have been carried out so far in the context of ZRP, but it would be interesting to study the general mass transport model discussed here with these additional generalizations. It would also be interesting to compute the distribution of maximal mass in PFSS where the condensate is sub-extensive. In this case, the extremal mass is not the total mass carried by the full condensate, but rather the site inside the condensate that carries the largest mass.

Acknowledgements: It is a pleasure to thank my collaborators in this subject: M. Barma, M.R. Evans, C. Godrèche, S. Gupta, T. Hanney, S. Krishnamurthy, R. Rajesh, E. Trizac and R.K.P. Zia. I also thank A. Comtet, D. Dhar, J. Krug, K. Mallick, H. Meyer-Ortmanns, D. Mukamel, G. Schütz and C. Sire for many useful discussions. This article is based on a series of lectures that I first gave at the summer school “The Principles of the Dynamics of Non-Equilibrium Systems” held at the Issac Newton Institute, Cambridge (2006) and later at the summer school “Exact Methods in Low-dimensional Statistical Physics and Quantum Computing” held at Les Houches (2008). I thank the organizers of both the schools for hospitality. The support from Grant No. 3404-2 of “Indo-French Center for the Promotion of Advanced Research (IFCPAR/CEFIPRA)” is also gratefully acknowledged.

-
- [1] S.N. Majumdar, S. Krishnamurthy and M. Barma, Phys. Rev. Lett. **81**, 3691 (1998).
 - [2] O.J. O’Loan, M.R. Evans and M.E. Cates, Phys. Rev. E **58**, 1404 (1998).
 - [3] D. Chowdhury, L. Santen and A. Schadschneider, Physics Reports **329**, 199 (2000).
 - [4] D. van der Meer, K. van der Weele and D. Lohse, Phys. Rev. Lett. **88**, 174302 (2002); J. Torok, Physica A **355**, 374 (2005); D. van der Meer et. al. J. Stat. Mech.: Theory Exp. P07021 (2007).
 - [5] Y. Kafri, E. Levine, D. Mukamel, G. M. Schütz and J. Török, Phys. Rev. Lett. **89**, 035702 (2002).
 - [6] Z. Burda *et al.*, Phys. Rev. E **65**, 026102 (2002).
 - [7] S.N. Dorogovstev and J.F.F. Mendes, *Evolution of Networks* (OUP, Oxford, 2003).
 - [8] M.R. Evans, Braz. J. Phys. **30**, 42 (2000).
 - [9] M.R. Evans, Europhys. Lett. **36**, 13 (1996).
 - [10] J. Krug and P.A. Ferrari, J. Phys. A: Math. Gen. **29**, L465 (1996).
 - [11] A.G. Angel, M.R. Evans, and D. Mukamel, J. Stat. Mech.: Theory Exp. P04001 (2004).
 - [12] F. Spitzer, Adv. Math. **5**, 246 (1970).
 - [13] M. R. Evans and T. Hanney, J. Phys. A: Math. Gen **38**, R195 (2005).
 - [14] C. Godrèche, Lecture notes for the Luxembourg summer school (2005), arXiv:cond-mat/0604276.
 - [15] P.L. Krapivsky and S. Redner, Phys. Rev. E **54**, 3553 (1996).
 - [16] S.N. Majumdar, S. Krishnamurthy, and M. Barma, J. Stat. Phys. **99**, 1 (2000).
 - [17] R. Rajesh and S.N. Majumdar, Phys. Rev. E **63**, 036114 (2001).
 - [18] R. Rajesh and S. Krishnamurthy, Phys. Rev. E **66**, 046132 (2002).
 - [19] E. Levine, D. Mukamel, and G. Ziv, J. Stat. Mech.: Theory Exp. P05001 (2004).
 - [20] R. Rajesh, D. Das, B. Chakraborty, and M. Barma, Phys. Rev. E **56**, 056104 (2002).
 - [21] D.J. Lee, S. Kwon, and Y. Kim, J. Korean. Phys. Soc. **52**, S154 (2008).
 - [22] V. Agarwal et. al., Phys. Rev. B **74**, 035412 (2006).
 - [23] P.K. Kuri et. al. Phys. Rev. Lett. **100**, 245501 (2008).
 - [24] E. Levine et. al. J. Stat. Phys. **117**, 819 (2004).

- [25] H. Yamamoto et. al. Japan J. of Industrial and Appl. Math. **24**, 211 (2007); A. Svorencik and F. Slanina, Eur. Phys. J. B **57**, 453 (2007).
- [26] S. Kwon, S. Lee, and Y. Kim, Phys. Rev. E **73**, 056102 (2006); *ibid* **78**, 036113 (2008); M. Tang and Z.H. Liu, Comm. in Theor. Phys. **49**, 252 (2008); D.Y. Hua, Chinese Phys. Lett. **26**, 018901 (2009).
- [27] J. Krug and J. Garcia, J. Stat. Phys. **99**, 31 (2000).
- [28] R. Rajesh and S.N. Majumdar, J. Stat. Phys. **99**, 943 (2000).
- [29] R. Rajesh and S.N. Majumdar, Phys. Rev. E **64**, 036103 (2001).
- [30] F. Zielen and A. Schadschneider, Phys. Rev. Lett. **89**, 090601 (2002).
- [31] C.-H. Liu et. al., Science **269**, 513 (1995); S.N. Coppersmith et. al. Phys. Rev. E **53**, 4673 (1996).
- [32] M.R. Evans, S.N. Majumdar, and R.K.P. Zia, J. Phys. A: Math. Gen. **37**, L275 (2004).
- [33] R.K.P. Zia, M.R. Evans, S.N. Majumdar, J. Stat. Mech: Theory Exp. **L10001** (2004).
- [34] S.N. Majumdar, M.R. Evans, and R.K.P. Zia, Phys. Rev. Lett. **94**, 180601 (2005).
- [35] M.R. Evans, S.N. Majumdar, and R.K.P. Zia, J. Stat. Phys. **123**, 357 (2006).
- [36] M.R. Evans, S.N. Majumdar, and R.K.P. Zia, J. Phys. A: Math. Gen. **39**, 4859 (2006).
- [37] E. Bertin, J. Phys. A: Math. Gen. **39**, 1539 (2006).
- [38] R.L. Greenblatt and J.L. Lebowitz, J. Phys. A: Math. Gen. **39**, 1565 (2006).
- [39] T. Hanney, J. Stat. Mech: Theory Exp. **P12006** (2006).
- [40] P. Bialas, Z. Burda, and D. Johnston, Nucl. Phys. B **493**, 505 (1997).
- [41] E.J. Gumbel, *Statistics of Extremes* (Columbia University, New York, 1958).
- [42] I. Jeon, P. March, and B. Pittel, Ann. Probab. **28**, 1162 (2000).
- [43] M.R. Evans and S.N. Majumdar, J. Stat. Mech: Theory Exp. **P05004** (2008).
- [44] M.R. Evans, T. Hanney, and S.N. Majumdar, Phys. Rev. Lett. **97**, 010602 (2006).
- [45] B. Waclaw, J. Sopik, W. Janke, and H. Meyer-Ortmanns, arXiv: 0901.3664.
- [46] B. Waclaw, J. Sopik, W. Janke, and H. Meyer-Ortmanns, arXiv: 0904.0355.
- [47] C. Godrèche, J. Phys. A: Math. Gen. **36**, 6313 (2003).
- [48] S. Grosskinsky, G.M. Schütz, and H. Spohn, J. Stat. Phys. **113**, 389 (2003).
- [49] C. Godrèche and J.M. Luck, J. Phys. A **38**, 7215 (2005).
- [50] S. Gupta, M. Barma, and S.N. Majumdar, Phys. Rev. E **76**, 060101(R) (2007).
- [51] G.M. Schütz and R.J. Harris, J. Stat. Phys. **127**, 419 (2007).
- [52] S. Gupta, S.N. Majumdar, C. Godrèche, and M. Barma, Phys. Rev. E **76**, 021112 (2007).
- [53] A.G. Angel and R.K.P. Zia, J. Stat. Mech.: Theory Exp. P03009 (2009).
- [54] S.N. Majumdar, S. Krishnamurthy, and M. Barma, Phys. Rev. E, **61**, 6337 (2000).
- [55] A.G. Angel, M.R. Evans, E. Levine, and D. Mukamel, Phys. Rev. E **72**, 046132 (2005); J. Stat. Mech.: Theory Exp. P08017 (2007).
- [56] S. Grosskinsky and G.M. Schütz, J. Stat. Phys. **132**, 77 (2008).
- [57] S. Grosskinsky, P. Chleboun, and G.M. Schütz, Phys. Rev. E **78**, 030101(R) (2008).
- [58] Y. Schwarzkopf, M.R. Evans, and D. Mukamel, arXiv:0801:4501 (2008).
- [59] M.R. Evans, S.N. Majumdar, E. Trizac, and I. Pagonabarraga, to be published.